BRNO UNIVERSITY OF TECHNOLOGY
VYSOKÉ UČENÍ TECHNICKÉ V BRNĚ

FACULTY OF ELECTRICAL ENGINEERING AND COMMUNICATION
FAKULTA ELEKTROTECHNIKY A KOMUNIKAČNÍCH TECHNOLOGIÍ

DEPARTMENT OF BIOMEDICAL ENGINEERING
ÚSTAV BIOMEDICÍNSKÉHO INŽENÝRSTVÍ

DETECTION OF HIGH-FREQUENCY EEG ACTIVITY IN EPILEPTIC PATIENTS

DETEKCE VYSOKOFREKVENČNÍ EEG AKTIVITY U EPILEPTICKÝCH PACIENTŮ

DOCTORAL THESIS – SHORT VERSION
DIZERTAČNÍ PRÁCE - TEZE

AUTHOR
AUTOR PRÁCE
Ing. Mgr. Jan Cimbálník

SUPERVISOR
ŠKOLITEL
Ing. Pavel Jurák, CSc.

BRNO 2016

ABSTRAKT

Tato práce se zabývá automatickou detekcí vysokofrekvenčních oscilací jakožto moderního elektrofyziologického biomarkru epileptogenní tkáně v intrakraniálním EEG, jehož vizuální detekce je zdlouhavý proces, který je ovlivněn subjektivitou hodnotitele. Epilepsie je jedním z nejčastějších neurologických onemocnění postihující 1% obyvatelstva. Přestože jsou přibližně dvě třetiny případů léčitelné farmakologicky, zbylá třetina pacientů je odkázána zejména na léčbu chirurgickým zákrokem, pro nějž je zapotřebí přesně lokalizovat ložisko patologické tkáně. Vysokofrekvenční oscilace jsou v posledním desetiletí studovány pro jejich potenciál lokalizace patologické tkáně. Součástí této práce je shrnutí dosavadního výzkumu vysokofrekvenčních oscilací a výčet detektorů používaných ve výzkumu. V rámci práce byly vyvinuty či vylepšeny tři detektory vysokofrekvenčních oscilací, na jejichž popis navazuje evaluace z hlediska shody s manuální detekcí, přesnosti výpočtu příznaků oscilací a schopnosti lokalizace patologické tkáně. V závěru práce jsou představeny vyvinuté metody vizualizace výskytu vysokofrekvenčních oscilací a stručně uvedeny dosažené vědecké výsledky.

KLÍČOVÁ SLOVA

Epilepsie, zóna počátku záchvatu, vysokofrekvenční oscilace, detekce vysokofrekvenčních oscilací.

ABSTRACT

This work deals with automated detection of high-frequency oscillations as a novel electrophysiologic biomarker of epileptogenic tissue in intracranial EEG. Visual detection of these oscillations is a time-consuming process and is prone to reviewer bias. Epilepsy is one of the most common neurological diseases affecting 1% of population. Even though two thirds of cases are successfully treated with anti-epileptic drugs, the rest of the patients are dependent mainly on surgical procedure, which requires precise localization of pathologic focus. High-frequency oscillations have been studied over the last decade for their potential to localize the focus of pathological tissue. Initial part of this work is a summary of the current state of high-frequency oscillations research and a detailed list of detectors used in research. Within the scope of this work three high-frequency oscillation detectors were developed or enhanced. The description of the algorithms is followed by detector evaluation with regard to the concordance with expert reviewed events, feature estimation and the ability to correctly localize pathological tissue. The final part of the work provides an overview of developed visualization methods and a short summary of achieved scientific results.

KEYWORDS

Epilepsy, seizure onset zone, high-frequency oscillations, detection of high frequency oscillations.

CONTENT

INTRODUCTION

Epilepsy is a group of diseases which affect the brain of the patients and significantly impairs their quality of life and limits them in their everyday activities. About 60% of epileptic patients can be treated with antiepileptic drugs, however, the remaining 30% of patients have to undergo a surgery to remove epileptogenic tissue causing their seizures. Even though the surgery is a highly invasive procedure the positive outcome is never guaranteed due to poor localization of pathological part of the brain.

Nowadays the localization of the epileptogenic focus is done by a number of methods, including scalp electroencephalography, magnetic resonance imaging and neuropsychologic examination. If the results of these examinations are inconclusive, the patient undergoes an electrode implantation to map the seizure onset zone in the brain. While seizure onset zone is located in majority of the cases, the resection of the tissue often does not bring seizure freedom to the patients. Thus, other biological markers of epileptogenic tissue, which would correctly localize the pathologic tissue, are essential for good outcome of the surgery.

High frequency oscillations (HFOs) in frequencies ranging from 80-600 Hz are a relatively novel and promising electrophysiological biomarker that could improve localization of epileptogenic focus and help the physicians minimize the resection area while achieving better surgery outcome and protecting the functional brain sites necessary for everyday life of the patient. Apart from being linked to the epileptogenic foci, they are also present in healthy brain during cognitive processing. Distinguishing between the physiological HFOs and pathological ones is one of current endeavors of neuroscientists.

Manual revision and marking of high frequency oscillations is a time consuming process and is prone to reviewer bias. Moreover, interviewer concordance is often poor leading to discrepancies in the analyses. Therefore, an objective, robust and fast method is needed to eliminate the drawbacks of visual detection. Development of such algorithm is hindered by an unclear HFO definition.

To date a number of detectors based on different HFO features and signal metrics have been developed but most of them were applied on preselected data sets or animal recordings solely for research work. Moreover, evaluation of the detectors is not uniform which makes them nearly impossible to compare.

The aim of this work is to develop and evaluate high-frequency oscillation detectors that are robust and feasible for clinical application and research. Such tools could provide physicians with valuable information about the patient's brain and could improve the well being of patients while reducing the costs of their stay in hospital. It also allows for studying HFOs in cognition and broadening the knowledge of brain processing.

Three detectors were developed or improved within this work. One based on well known line-length metric, second which uses a novel frequency homogeny metric to overcome effects of Gibb's phenomenon and third based on normalized Hilbert transformed signals.

All detectors were evaluated from three different perspectives. Agreement between human scored events and automated detection was evaluated using precision-recall analysis. Correctness of feature estimation was assessed with the use of artificial events and comparison of their set features with automatically computed features. Lastly, the ability of the detectors to correctly localize pathological tissue was measured using pathological channels marked by expert reviewers and resected areas in patients with good surgical outcome.

To provide clinicians and researchers with information about HFO occurrence and their features three visualization methods developed for this purpose are presented. One is based on HFO rates in individual frequencies, other uses MRI scans to simultaneously provide information about the anatomy of the studied brain and the last one providing information about HFO rates, their features and brain connectivity.

The results of this work are currently being used in St. Anne's University Hospital in Brno, Czech Republic and Mayo Systems Electrophysiology Laboratory at Mayo Clinic, USA. Further work will focus on algorithm optimization, on-line implementation and HFO clustering.

1 FOCAL EPILEPSY, ITS TREATMENT AND DIAGNOSTICS

Epileptic seizures and epileptic syndromes have high prevalence and incidence rates affecting both sexes, all ages and all races. Their estimated incidence ranges between 0.5% and 1% [1]. They constitute an important part of everyday neurological practice and are listed among the most frequent neurological diseases along with Parkinson's and Alzheimer's disease.

The ultimate aim of epilepsy treatment is total seizure freedom with no clinically significant adverse effects. The majority of epilepsies are successfully treated with anti-epileptic drugs (AEDs) in continuous prophylactic schemes with drug mixtures tailored to each patient. However, AEDs are ineffective for about 20% of epileptic patients. These patients are candidates for neurosurgical interventions, other pharmacological or non-pharmacological treatments.

A successful surgical intervention requires the epileptogenic tissue to be well localized, and located in the brain area that can be removed safely without significantly impairing the normal function of the brain. The correct localization of the pathological tissue is often crucial for the surgery to have a good outcome by achieving seizure freedom for the patient. Despite the development of neuroimaging diagnostic methods, additional information is often needed to better localize the focus of epileptic seizures. This information is provided by the intracranial EEG (iEEG) which involves highly invasive, albeit necessary, craniotomy procedure or access to the brain through drilled holes in the skull and implantation of depth or/and subdural electrodes.

Apart from intracranial EEG other medical technologies have an increasing impact on diagnosis and treatment in epilepsy where the use of technologies is inevitable due to relative inaccessibility of the brain. Nowadays epileptologists have a wide array of methods to choose from. The neuropsychological testing serves for determination of cognitive brain areas which might be affected by epilepsy. Video-EEG is capable of capturing patients behavior along with EEG recording which helps to map all cognitive deficiencies. Neuroimaging techniques serve for detection of anatomical and histological brain abnormalities as well as changes in brain metabolism.

2 HIGH-FREQUENCY OSCILLATIONS

High-frequency oscillations (HFOs) are electrophysiological phenomena visible in intrcranial EEG signals with frequencies above the usual clinical range of analysis, so called Berger bands [2]. Since their initial description in 1992 [3] HFOs have been intensively studied as biomarkers of epileptogenic tissue and as signs of cognitive functions.

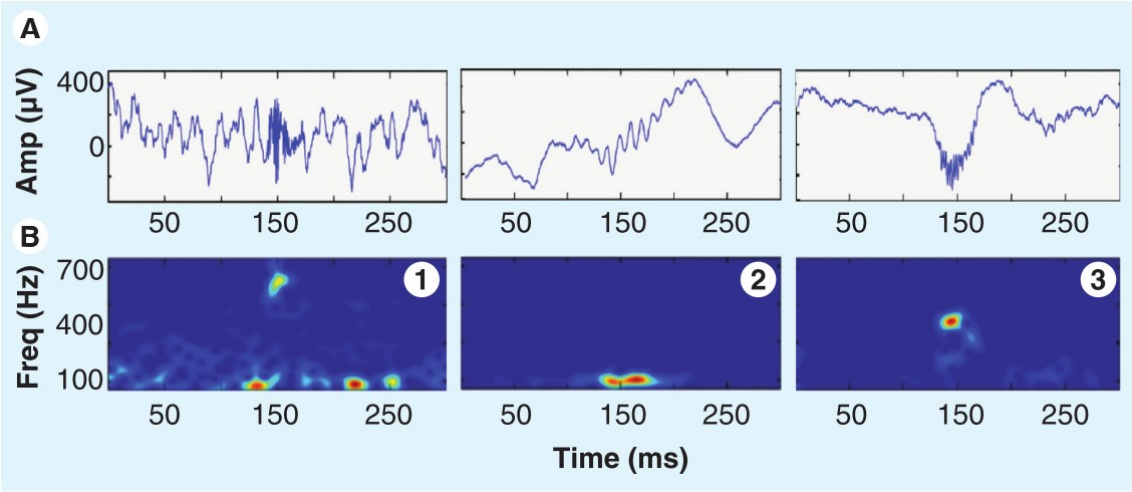

Figure 1: ***Representative examples of HFOs.***

Each plot shows two views of HFOs in 300ms window: (A) unfiltered iEEG with an HFO located in the center ~150 ms, (B) spectrogram (2.6 ms window). (1 & 3) Typical HFOs in fast ripple range. (2) Typical HFO in ripple range. Amp: Amplitude, Freq: Frequency [2].

HFOs were first described in hippocampus of freely behaving rats as a physiologic phenomenon. They were named ripples with their frequency band ranging from 80-200 Hz [3]. Later, the same group of scientists described another type of HFOs in epileptic rats which were called fast ripples due to their high frequency bands 200-600 Hz. Similar to the model of epileptic rats both ripple and fast ripple oscillations were identified in human epileptogenic hippocampus. A typical HFO appearing in iEEG signal is depicted in Figure 1 [2]. Some recent studies also suggest that HFOs are occurring at frequencies above the FR range (> 1000 Hz) but are deemed to be a different pathophysiological phenomenon [4].

2.1 CURRENT STATE OF HFO RESEARCH

Ranging from 80 to 600 of cycles per second, high frequency oscillations are likely to bridge the local action potential firing of individual neurons with the large-scale interactions of neuronal networks. Studies of HFOs in cognition have largely focused on frequencies of the gamma range up to 120Hz which overlaps with the reported ripple frequencies. Nevertheless, neuronal interactions are known to extend beyond the classic gamma oscillations, e.g. synchronous firing of neuronal populations was shown to correlate most strongly with the 80-200Hz frequencies [5].

Much less is known about the roles of HFOs in the ripple, fast ripple and novel very high-frequency oscillations bands (125-1000Hz) during cognition. The underlying mechanism of ripple is believed to be discharges of synchronized firing between specific neuronal ensembles, mainly occurring during states of rest and sleep [3]. In sleep, ripples were shown to comprise sequential firing of specific hippocampal assemblies that were active during preceding behavior in rats [6]. Interestingly, ripples were shown to be generated by the same neuronal networks and mechanisms as the gamma oscillations [7]. Whether the human ripple-frequency HFOs support the same function as the hippocampal sharp-wave ripple complexes in rodents remains to be established, as well as the role of cortical oscillations in the ripple frequencies.

HFOs have been investigated in number of human studies, all of which confirmed the link between higher HFO rates and pathologic brain [8][9][10][11][12][13][14][15][16][17]. Unlike spikes which are deemed to be another biomarker, HFOs have been proven to better localize pathological tissue [13]. Studies investigating the relation of post surgical persistent seizures and areas with present pathological HFOs showed a better surgical outcome when the area of the brain with HFOs was resected [18][19]. All of these studies, however, evaluated HFOs only in limited number of patients (~10) and/or reviewed only short segments of iEEG which lowers their statistical power. Most of the studies are also based on visual identification of HFOs which is a time consuming process, can introduce human bias into the results and is not feasible for large data sets. Lastly, results of HFO studies are often reported relative change of HFO rate in SOZ rather than absolute HFO rates which are not suitable for prospective studies, thus cannot be translated into clinical environment.

3 CURRENT STATE OF HIGH-FREQUENCY OSCILLATION DETECTION

Generally the detection of a graphical element in a signal requires definition of its features. The features can differ significantly based on anatomy or whether the tissue is pathologic or not [20].

The three most obvious and most common features used in EEG processing are amplitude, duration and frequency. HFOs are a short-duration, high frequency events standing out from the background so all these features can be utilized for their detection.

3.1 HFO DETECTORS DEVELOPED TO DATE

Every detector designed to date utilizes a method that preprocesses the signal by applying frequency filters, calculates the energy of the filtered signal and pick candidate events as those exceeding the set statistical threshold.

The detector designed by Staba et al. adopted the moving average of root mean square of the preprocessed signal as the energy metric [10]. The preprocessing stage involves band-pass filtration of iEEG signal (100-500 Hz). The metric threshold was set to 5 standard deviations above the mean of the whole signal. Events shorter than 6ms were disregarded and events less than 10ms apart were regarded as one HFO. The reported sensitivity of this algorithm was 84%. The algorithm was originally developed for micro-electrode recordings in rats and humans.

Nelson et al. [21] suggested a detector using the energy metric called Teager energy which was initially designed for applications in acoustics [22]. In their experiment the signal was filtered by a Butterworth filter, however, the cut off frequencies were not reported even though the frequency setting is crucial. No sensitivity or specificity results were provided. The Teager energy metric was suggested for rat micro-wire recordings.

Gardner et al. [23] developed a detector based on line length of the iEEG signal originally designed for detection of high-gamma events and subsequently used for HFOs [12]. In the preprocessing stage the signal was filtered by a Butterworth band pass filter (30 – 100 Hz [23], 80 – 1 kHz [12]). The statistical threshold was set to 95 percentile of the given

statistical window (3 minutes). The sensitivity of this detector was reported to be 89.5 % [23]. The recordings for which this detector was designed were micro as well as macro-electrode human iEEG [23].

Amplitude envelope of filtered iEEG signal calculated by Hilbert transform was used in semi-automated detector designed by Crepon et al. [17]. The band pass filter used in preprocessing was set to 180 – 400 Hz. HFOs were detected as 5 SDs of iEEG signal amplitude. The detector was developed for HFO detection in human macro-electrode recordings.

In contrast with the previously described algorithms Zelmann et al. [24] created an algorithm that uses previously detected background activity to calculate the signal statistics. The filter settings were confined to the band pass 80-450 Hz. The threshold for putative HFO detection is calculated as the 95 percentile of the cumulative distribution function of the previously detected background segments. The reported detector sensitivity was 96.8 +/- 8.91% and specificity 99.1 +/- 8.91%. The target recordings were human macro-electrodes.

A detector based on some of the metrics used in previous works. The detector aims on detection in ripple band only, meaning that the frequency band in which it operates is 80 – 250 Hz. It utilizes signal energy, line-length and instantaneous frequency. These metrics are processed by a radial basis function neural network. The reported sensitivity was 49.1% and specificity 36.3 % [25].

An online detector proposed by Lopez-Cuevas et al. [26] uses metric of signal complexity (Approximate entropy [27][28]) rather than signal energy. After calculation of approximate entropy of raw signal an artificial neural network was trained to detect HFOs with 4 neurons in the initial layer using last 4 values of approximate entropy as their inputs. This algorithm was designed for micro-electrode rat recordings.

The algorithm designed by Sahbi-Chaibi et al. [29] uses part of Hilbert-Hunag transform and its integral part empirical mode decomposition (EMD) for HFO detection. Firstly the intrinsic mode functions (IMFs) are acquired using EMD. Instantaneous frequency and amplitude is calculated in each IMF with Hilbert spectral analysis. Because instantaneous frequencies are sensitive to noise, smoothing is applied to circumvent this drawback. Subsequently instantaneous amplitude coefficients are accumulated only in function of IMFs traces presented in HFOs band 80-500 Hz. The obtained 1-D signal is smoothed by root mean square operation and thresholded for detection of HFOs.

The method for detection of FR in iEEG created by Birot et al. uses frequency band of 256 – 512 Hz, which was chosen for methodological reasons. First, the signal energy is obtained by calculating line-length. After thresholding, the putative HFOs are further processed by either Fourier transform or wavelet transform, where the ratio between FR frequency band and lower frequency band is calculated. This metric is further thresholded and the final HFO detection is obtained. The reported sensitivity and specificity were not reported, however, the best AUC achieved was reported to be 0.983 and 0.986 for the Fourier transform method and wavelet transform method respectively. [30].

Capable of detection in both ripple and fast-ripple frequency range the detector proposed by Burnos et al. utilizes Stockwell transform. During first stage of the algorithm the signal is filtered and amplitude envelopes are calculated using Hilbert transform. Such signal is thresholded with low threshold setting to detect putative HFOs with high sensitivity. The putative HFOs are further processed by Stockwell transform. The power spectral density was used to distinguish between HFO detections and putative detections produced by Gibb's phenomenon, such as artifacts and spikes [31]. The sensitivity and specificity was evaluated for each recording separately, and average values were not calculated.

4 AIMS OF DISSERTATION

The main goal of this work was development and validation of automated HFO detectors, study of HFOs in patients suffering from intractable epilepsy and localization of epileptogenic zones within pathologic brain. Apart from the main focus on automated detection algorithms, HFO occurrence analyzes were carried out and result presentation tools were created within this work. The main analyzes and methods that may in the future contribute to basic research of the brain as well as improved diagnostics are listed below:

- Fast and robust algorithms for detection of high-frequency oscillations and their validation with regard to gold standard data sets as well as SOZ and resected area in patients with good surgical outcome.
- Modular software tools to validate any HFO detection algorithm.
- Characterization of HFOs with regard to the behavioral state of the patient, anatomical structure, type of epilepsy, etc.
- Software tools to detect HFOs close to real-time detection with a lag approximately 10s make it possible to view HFO occurrence inside the operation room to evaluate the feasibility of such approach to map and resect the epileptogenic focus in one procedure.
- Tools to present HFO occurrence in a comprehensive form for physicians.

The ultimate gold of this work is to provide physicians with additional information about HFO occurrence, and thus, better localize pathological tissue in patients with pharmacoresistant focal epilepsies and improve the outcome of the brain surgery, therefore life and well-being of the patients.

5 DEVELOPED AND IMPROVED ALGORITHMS

Three detectors of HFOs were used within the frame of this work. Each of the detectors was developed for different definitions of HFO and distinct purposes. This section is divided into three chapters each describing the algorithms, their purposes, advantages and disadvantages. All HFO detection algorithms can generally be divided into three stages: pre-processing, detection, post-processing. All of these stages are described in individual sub-sections.

5.1 LINE LENGTH DETECTOR WITH FEATURE CASCADE

This algorithm was developed to analyze enormous data sets produced by long term clinical iEEG recordings (TB of data). The main purpose was to retrospectively evaluate the relationship between the pathological brain and HFO rates recorded with iEEG electrodes. The core of this algorithm, i.e. the processing part was developed by Benjamin H. Brinkmann (MSEL). The main advantage of the line-length metric is that it reflects increases in both signal amplitude and frequency. However, it is dependent on sampling frequency and prone to presence of noise in the signal. The algorithm was already used in number of works [23, 30, 32, 33].

In the pre-processing stage the signals are usually visually checked for excessive noise levels or even channels that include no useful signal. These channels are excluded from the analysis. The rest of the channels are filtered with a band-pass 4-pole butterworth filter to 100-600 Hz frequency band. In the detection stage a 10s statistical window is created and the filtered signal is converted to line-length signal (Equation 1), using 50ms (5 oscillations at 100 Hz) sliding window with ¼ overlap. These parameters can be varied as needed. Mean and standard deviation are calculated and a fraction of standard deviation above the mean is used as a threshold. The threshold is set so that the sensitivity of this step is 100%. The possible danger here is that if signal-to-noise ratio is low, the noise can increase overall line-length metric and the HFO is not detected because it does not stand out from the background. Conversely, if the threshold is set too low, the signals that are less active yield more detections than active channels. This happens due to higher line-length standard deviation in active channels.

$$LL = \sum_{k=t-N+2}^{t} \left| (x_k - x_{k-1}) \right|$$

Equation 1: Line-length metric.

The post-processing stage was added within this work and it involves calculation of HFO features – duration, amplitude, frequency (using multi-taper power spectral density) and event to background ratio and correlation with low-passed signal for improvement of algorithm specificity.

5.2 ALGORITHM BASED ON FREQUENCY HOMOGENY

The purpose of this algorithm was to be able to process large datasets while improving specificity compared to less sophisticated methods. Originally designed by Mathew Stead (MSEL) the algorithm efficiently removes false positive HFO detections that occur due to Gibb's phenomenon while maintaining reasonable speed of detection.

In the first step the signal is filtered with band pass butterworth filters in a sequence of overlapping frequency bands that cover the whole frequency span of high-frequency oscillations (80 – 600 Hz). Each filtered band is processed separately in the subsequent steps in the same fashion.

First, the amplitude envelope of the filtered signal is calculated using Hilbert transform (Equation 2).

$$F(t) = \frac{1}{\pi} \int_{-\infty}^{\infty} \frac{f(x)}{t - x} dx$$

Equation 2: Hilbert transformation.

Second, a metric evaluating frequency stability is calculated as the “signal-to-noise” ratio (Equation 3). The numerator of the equation is the root mean squared cosine representation of the narrow-band signal phase (Equation 4) and the denominator is the root mean squared difference between the cosine representation of the broad-band and narrow-band filtered signal phases (Equation 5). The broad-band filtered signal has the same cut-off frequency as the narrow-band passed signal but the low cut-off frequency is four times smaller. This second metric servers for elimination of detections caused by higher amplitude in filtered signal which is produced by Gibb's phenomenon.

$$SNR_j = \frac{\sqrt{npxx_j}}{\sqrt{bpxx_j}}$$

Equation 3: Frequency homogeny metric.

where

$$npxx_j = npxx_{j-1} - np_i^2 + np_k^2$$

Equation 4: Frequency homogeny numerator.

and

$$bpxx_j = bpxx_{j-1} - (bp_i - np_i)^2 + (bp_k - np_k)^2$$

Equation 5: Frequency homogeny denominator.

The third step of metric calculation consists of calculating the dot product of the normalized signal amplitude envelopes and frequency stability metric, thus obtaining a signal that utilizes both amplitude and frequency features of the analyzed signal. If one of the metrics is negative the resulting signal is put to 0.

To account for non-stationary character of EEG signal all metrics are normalized by Poisson normalization. The detection of putative HFOs is done by thresholding the normalized product metric. Each putative HFO enters the cascade of minimum and maximum value boundary thresholds for amplitude, frequency stability, dot product and duration. The thresholds are calculated from cumulative distribution functions that were generated from the features of HFOs visually marked by expert reviewers.

5.3 HILBERT 2D DETECTION ALGORITHM

The algorithm was developed to detect physiological HFOs occurring during cognitive and memory tasks and to broaden the understanding of pathological HFOs with regard to their features. The aim of this algorithm is to provide detailed study of individual pathological and physiological HFO features, and thus contribute to the distinction between the two groups and their behaviors.

Instead of using a wider frequency band of interest, such as 80 – 600 Hz this algorithm uses a series of band passed signals using 4-pole butterworth filter. This can be achieved by band-passing the original signal with 1 Hz step. Z-score for each signal is calculated. (EQ) Such approach can be visualized in a time-frequnecy matrix. This matrix differs from classical time-frequency analysis in three aspects. The produced matrix does not use sliding windows so each sample corresponds exactly to the sample of raw signal. Furthermore, each band reflects changes in amplitude rather than power of the band, result of which is that baseline noise, such as 60 Hz, is not visible in the matrix. Finally, the 1/f characteristic of EEG is overcome by individual z-score normalization of each band.

$$\text{z-score} = \frac{x - \bar{x}}{s_x}$$

Equation 6: Standard score (z-score) calculation.

As it is apparent from the higher frequencies of the histogram carry redundant information. Therefore, choosing a logarithmically spaced frequency bands is a logical approach to reduce the information redundancy and increase algorithm speed. The logarithmically spaced equivalent is depicted in.

In order to overcome the consequences of Gibb's phenomenon the cross correlation is calculated between band-passed signal and the low-passed signal with the common high cut-off frequency. To speed up this calculation the relationship between convolution and correlation is exploited (Equation 8) and convolution is done by multiplication in the frequency domain (Equation 9). The cross correlation signals can be again visualized in a matrix.

$$corr\left(x[n], h[n]\right) = \sum_{k=0}^{\infty} h[k]\, x[n+k]$$

Equation 7: Correlation

$$x[n] * h[n] = \sum_{k=0}^{\infty} h[k]\, x[n-k]$$

Equation 8: Convolution

$$f(x) * f(h) = F(x) \cdot F(y)$$

Equation 9: Convolution in frequency domain.

To create a metric that takes into account both amplitude and cross correlation the square root of the dot product is calculated.

The detection of events is done by thresholding the final metric in each frequency band. Since the metrics are z-scored, the used threshold represents a fraction of standard deviation above the mean. The detections with less than one cycle period apart in one frequency band are joined into one event. The detections in different frequency bands overlapping in time domain are joined into a single HFO detection.

Only one post-processing step is applied to reduce the number of false positive detections. The number of cycles is calculated using event peak frequency and duration and the events that are shorter than 1 cycle are discarded. The detections then enter a cascade of feature calculations.

6 DETECTOR EVALUATION

To quantify the efficiency of HFO detection algorithms they have to be evaluated. Even though each publication of HFO detection algorithm method contains some form of efficiency quantification the methods for detection evaluation are not unified which makes a direct comparison almost impossible. This chapter presents the methodology and results of algorithm evaluation used in this work.

6.1 USED EVALUATION METHODS

Since each detector was developed under slightly different conditions and for varied purposes the results acquired for the given data set might not correspond to the results when applied to data sets that have, for example, different montage.

6.1.1 Analysis based on gold standard data sets

Acquisition of the gold standard detections was done separately by two expert reviewers in iEEG signals from 5 minute segments in 3 patients. 9 channels per patient were evaluated; 3 channels were localized in SOZ, 3 in IZ and 3 in nonSOZ area of the epileptic brain which was previously selected by epileptologists in clinical recordings. The HFOs were marked as segments of filtered signals that had 4 times higher amplitude than the surrounding signal and the amplitude spanned at least 4 cycles. To eliminate false detection produced by filter ringing care was taken to review the detection in the raw signal for sharp transients. Only the detections where both reviewers agreed were considered true positives.

Evaluation was carried out for detected events without any correction and for detections with visually excluded noisy segments.

Numbers of true positive, false positive and false negative detections were collected and precision-recall characteristics were calculated and plotted. Numerical evaluation was done by calculating F_1, F_2, and $F_{0.5}$ measures that can be found in the full version of the thesis.

6.1.2 Analysis based on feature estimation precision

To evaluate the feature estimation of the detectors, artificial HFOs were inserted into 20 minute long iEEG signal, which was previously visually checked for absence of visible HFOs. The used signal was taken from a contact located in white matter to avoid muscle artifacts and possible

contamination by physiological HFOs from neocortex or structures of lymbic system. Furthermore, the signal was visually checked for any signs of pathologic activity and artifacts. The artificial events in form of simulated spikes, HFOs, delta functions, line noise and HFO-spikes (HFOs coincident with spikes), were inserted in 3 second intervals with varying amplitude, frequency and duration. To assess the influence of event amplitude on feature estimation the signals with artificial events were created for different amplitudes separately with the values spanning from 0.1 to 0.5 std (0.1 std step) of iEEG signal amplitude. In order to to investigate whether noise produces any distortion in feature estimation, separated analysis was conducted on signals with superimposed pink noise, which is typical for EEG. All algorithms were run with the lowest threshold settings to achieve the highest sensitivity possible.

This analysis is somewhat limited by the detection methodology. In case of the line-length detection algorithm the amplitude and frequency have to be computed in post-processing steps because it utilizes only one frequency band and the line-length metric takes both features into account. Frequency homogeny algorithm uses rigid frequency bands thus a priori creates error in the estimation of this feature.

6.1.3 Analysis of HFO rates with regard to localization of pathologic tissue

A sample of 30 minute recordings from 5 patients was processed by automated detectors developed and modified in this work. Clinical recordings were reviewed by experienced epileptologists and seizure onset zone, irritative zone and normal channels were marked. Irritative zone was marked within the channels that had clear pathologic activity. Determination of resected area and subsequent channel marking was done by experienced clinicians using overlapped pre and post-surgical MRI. Surgery outcome was evaluated based on Engel class. Four patients had favorable outcome of Engel IA while one had persisting seizures with outcome Engel IIIA.

The detection was done by all algorithms for varying threshold settings and best performing threshold was determined using the lowest p value (t-test). ROC for each detector was constructed using either SOZ, SOZ+IZ or resected channels as targets, the varying variable was HFO rate. To compensate for potential differences in patients the same analysis was done for per patient normalized rates. The AUC were calculated for each ROC

separately to evaluate pathologic tissue localization.

6.1.4 Analysis of algorithm speed

All algorithms were run on one channel of itracranial EEG data with the length of 30 mins and 5 kHz sampling frequency. Standard desktop computer unit was used for evaluation with 12 GB RAM memory and Intel® Xeon(R) CPU E5-1620 0 @ 3.60GHz × 8 processors. Algorithms were all implemented in Python programming language.

6.2 RESULTS

Automated HFO detection is a complex task that is still being actively developed. Individual detection methods vary in HFO definition, the purpose for which they were developed and the datasets on which they were tested. This makes the comparison across multiple institutions difficult. The detection methods created in this work do not suffer from these problems because they are tested on the same datasets and evaluated by uniform methods.

6.2.1 Results of comparison with gold standard detections

Construction of precision-recall curves proved that frequency homogeny algorithm achieved the best performance at detecting human scored events with the lowest F scores.

The performance of line-length detector proves the usefulness of this algorithm in HFO detection. The reasonable performance shows that this method is robust, albeit simple.

Hilbert detector exhibits poorest performance regarding agreement with gold standard detections.

Similar analysis with semi-automated approach, where noisy segments in the data were marked by reviewers and all detections in these areas discarded, was performed. All detectors showed improved performance (Figure 2).

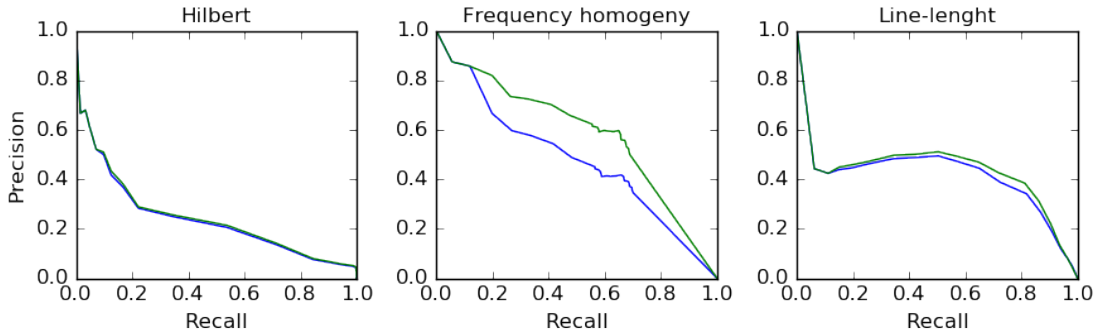

Figure 2: ***Precision-recall analysis of gold standard HFO detection.***

Precision-recall curves of agreement with gold standard reviewer marks. Blue – automated detection, green – semi-automated detection.

6.2.2 Results of feature estimation precision

The analysis of amplitude estimation precision revealed that all algorithms overestimated event amplitude (Table 1). Increased amplitude of simulated events showed improved mean amplitude estimation error in all detectors, however, the standard deviation increased. The best performing algorithm for this feature was the Hilbert detector while frequency homogeny and line-length detectors showed similar results.

		STD fraction				
Feature	Algorithm	0.1	0.2	0.3	0.4	0.5
Amplitude	FH	2.033	1.488	1.751	1.755	0.761
	Hilbert	1.704	1.213	1.371	1.415	0.632
	LL	2.366	1.564	1.717	1.609	0.664
Duration	FH	0.009	0.011	0.011	0.012	0.011
	Hilbert	-0.001	0.001	0.002	0.003	0.002
	LL	0.095	0.096	0.104	0.097	0.095
Frequency	FH	-6.526	-11.126	-14.242	-10.71	-17.863
	Hilbert	-0.091	-8.234	-6.193	-4.917	-6.342
	LL	-212.206	-189.411	-148.561	-92.388	-93.625

Table 1: ***Mean feature differences from artificial HFO events.***

Similarly to amplitude, all algorithms exhibited overestimation of duration (Table 1). Changes in artificial event amplitude did not have any impact on duration estimation. The Hilbert algorithm was the best performing while the worst was line-length algorithm.

Contrary to amplitude and duration all algorithms underestimated frequency irrespective of the event amplitude (Table 1). Increasing event amplitude worsened frequency estimation in Hilbert detector and frequency homogeny detector only in transition between the lowest threshold setting to the second lowest setting. The most precise algorithm was the Hilbert algorithm and the worst was the line-length algorithm.

In general, Hilbert algorithm showed best performance in analysis of feature estimation. Frequency homogeny algorithm performed roughly similarly to line-length detector in amplitude estimation but was worse in duration and frequency estimation. Line-length algorithm had poorest performance in feature estimation. Noise in signal had the highest impact on amplitude estimation. Duration and frequency showed similar mean differences as the signal without noise.

6.2.3 Results of pathologic tissue localization

Investigation of pathological tissue localization with regard to detector threshold revealed a trend for line-length detector where higher thresholds improved localization both in normal vs. pathological (SOZ + IZ), normal vs. SOZ analysis (disregarding IZ) and resected channels in patients with good outcomes (Table 2).

Threshold analysis of pathological tissue localization revealed that line-length and Hilbert algorithms showed a similar trend where increasing threshold led to improved detection. Contrary to the other two algorithms frequency homogeny detector had inverse trend where the lowest threshold achieved the best results. The best performing thresholds were 5, 0.1, 5 for line-length, frequency homogeny and Hilbert algorithms respectively.

ROC curves for best performing thresholds were done for pathology, SOZ and resected channels as target instances (Table 2 and Figure 3). Line-length detector had the highest values of AUC for pathology and SOZ analysis. Hilbert detector had the highest AUC for resected channels.

Using per patient normalized HFO rates generally improved performance of all HFO detectors.

Algorithm	Feature	Pathology	Seizure onset zone	Resection
Line-length	HFO count	0.778	0.951	0.704
	normalized HFO count	0.783	0.957	0.709
Hilbert	HFO count	0.537	0.787	0.719
	normalized HFO count	0.613	0.822	0.803
Frequency homogeny	HFO count	0.565	0.628	0.637
	normalized HFO count	0.593	0.584	0.752

Table 2: ***AUC values for pathological channel localization.***

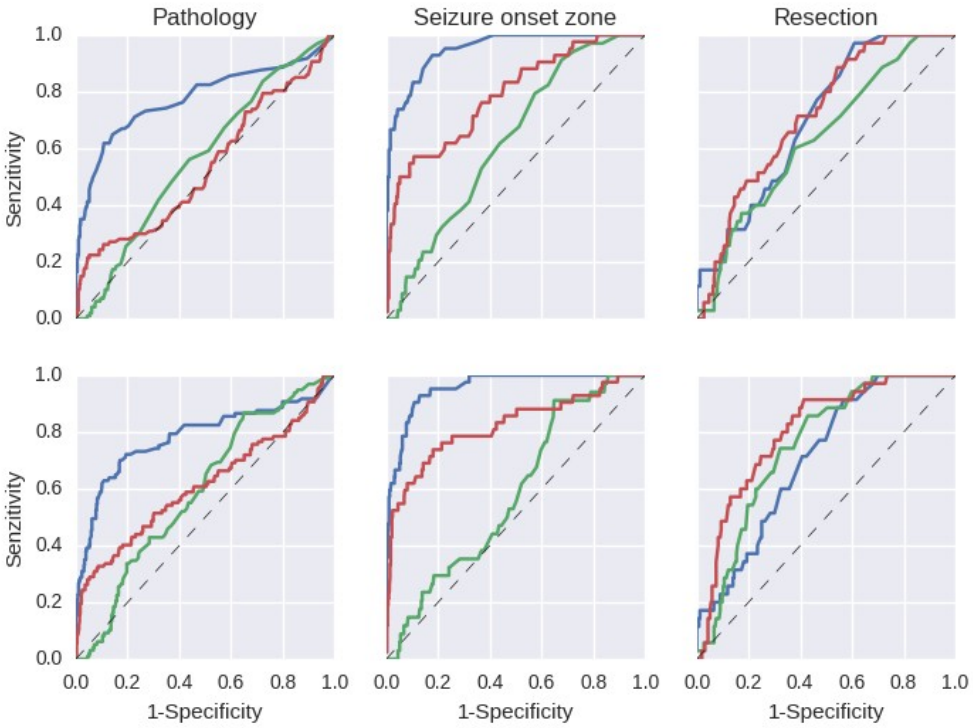

Figure 3: ***ROC analysis of pathologic tissue localization.***

ROC curves for localization of pathological tissue. Line-length algorithm outperforms the other two in clinically determined channels (Pathology, Seizure onset zone) but is the worst in determination of resected channels in patients with good outcome. Hilbert algorithm shows the best performance in this regard. Top – ROC for HFO rates, bottom – ROC for per patient normalized HFO rates. Blue – line-length, green – frequency homogeny, red – Hilbert.

6.2.4 Algorithm speed results

The fastest algorithm was the line-length based detector which processed the dataset in 265 s which is 6.79 times faster than real time (30 mins). The second algorithm was the frequency homogeny with the computation time of 1592 s which is 1.13 times faster than real time. The slowest algorithm was the Hilbert detector with the processing time of 7840 s and 0.23 times slower than real time.

6.3 SUMMARY OF RESULTS AND DISCUSSION

Four types of evaluation were performed: ability of detectors to correctly detect gold standard HFOs marked by expert reviewers, ability to correctly estimate HFO features, ability to correctly localize tissue that exhibits pathologic electrophysiologic activity (SOZ+IZ), seizure onset zone (SOZ) or resected channels in patients with good surgical outcome and processing time of each algorithm.

Evaluation of detector performance based on expertly reviewed events is often used in scientific literature dealing with HFO detection [29, 31, 32]. Within the scope of this work the best performing algorithm was the one based on the frequency homogeny metric. This result confirms the assumption that the algorithm improves specificity compared to earlier and simpler detectors such as line-length and RMS detector [10, 23]. Higher specificity can be explained by the novel metric which effectively eliminates Gibb's phenomenon as well as to post-processing steps that take reviewer expertise into account.

The second best performing algorithm was the line-length algorithm with added simple post-processing steps. The results in this work corroborate previous findings in earlier studies [23, 32]. The fact that the specificity is lower might reflect insufficient elimination of Gibb's phenomenon with use of correlation and detection of events that are not visible for naked human eye.

The design and purpose of the algorithm based on Hilbert envelopes, which is feature extraction while maintaining high sensitivity, was reflected in very poor specificity. This confirms that post-processing steps or methods of machine learning have to be applied in order to achieve better concordance with human reviewers.

Results of the same analysis performed in semi-automated fashion where noisy segments were removed by reviewers improved in all tested

algorithms. The highest improvement by 0.07 in F_1 score was seen in frequency homogeny algorithm. This suggest that either a manual or automated detection of noise and artifacts can lead to a substantial increase in performance.

The feature estimation aspect of detectors was evaluated using artificial HFO events with known amplitude, frequency and duration that were inserted into one channel of non-pathologic iEEG signal. Increasing event amplitude was applied to estimate change in feature estimation error.

All algorithms showed trend to overestimate the amplitude. This could be ascribed to the noise of the original iEEG signal into which the artificial signals were inserted. Increased amplitude of simulated events showed improved mean amplitude estimation in all detectors which is likely due to higher signal to noise ratio but the standard deviation of the estimation error increased presumably because of high amplitude of spikes in HFO-spike artificial events. The Hilbert algorithm showed the best performance which is likely due to precise detection of event onset and offset.

Analysis of duration estimation precision revealed the same trend as with amplitude where all algorithms overestimated this feature. This could be caused by algorithm methodology, which is further discussed below, and by filtration that smears the extent of the event to some extent. The worst performing algorithm was the line-length based algorithm while the Hilbert algorithm showed the best performance. These results stem from the algorithm nature since line-length algorithm utilizes sliding window with only 25% overlap it introduces error into duration estimation. Contrarily, Hilbert algorithm uses sample by sample detection leading to higher precision. Frequency homogeny algorithm introduces estimation error likely due to the sliding window nature of frequency homogeny metric.

Frequency estimation showed inverse trend to those of duration and amplitude and all algorithms underestimated frequencies of simulated events which could be ascribed to frequency band sequences used by these detectors. Hilbert detector and frequency homogeny detector showed stable frequency estimation with increasing event amplitude which worsened only in transition between the lowest threshold setting to the second lowest setting. The possible cause here is the more precise detection of event onset and offset with lowest threshold settings. The frequency calculation in line-length algorithm is done by detection of the maximum peak in frequency spectrum leading to a substantial error which, however, diminishes with event amplitude where the maximum spectrum peak is more prominent.

In summary, the Hilbert detector outperformed the other two detectors in estimation of all evaluated features. This result confirms that the Hilbert detector design is the most suitable tool for in depth study of HFOs. Frequency homogeny algorithm performance exhibited reasonable estimation error proving that it can be used for rough overview of HFO features in the detected dataset. Line-length detector showed the poorest performance which is due to the simplistic nature of the algorithm.

The capability of pathological tissue localization is vital for clinical applications. This is often tested in the literature along with analysis of successful detection of gold standard detections [24, 30, 31]. While this approach is the most important in clinical applications the best performance in this regard does not necessarily mean that the algorithm can as efficiently serve for basic research of HFO.

All algorithms were able to successfully show increased HFO activity in pathological tissue based on HFO detection. Relatively high thresholds in line-length and Hilbert detector showed the best performance with regard to SOZ localization. This can be explained by the core of these algorithms which is based mainly on signal amplitude. Frequency homogeny algorithm showed the best performance in the lowest threshold setting.

Analysis of tissue generating pathological interictal epileptiform spikes and HFOs (SOZ+IZ) decreased the performance of all algorithms. HFOs have been proved to be more localized in SOZ [9], thus this finding corroborates these previous results.

Analysis of HFO rates in patients with good surgical outcome showed improvement in frequency homogeny and Hilbert algorithm while decreasing the performance of line-length algorithm. The result highlights low specificity of line-length algorithm suggesting that it might be influenced by false positive detections of spikes.

ROC curves were created with the best performing threshold of each algorithm with HFO rate in individual channels as the threshold metric and pathological channels as targets. Interestingly, the line-length algorithm showed the best performance in SOZ localization while frequency homogeny the worst. Hilbert algorithm showed the best localization of resected channels. When the HFO rates were normalized on the per patient bases the results improved for resected channels in patients with good outcome suggesting that HFO rates may vary depending on implantation sites and patient's brain.

Processing time for each algorithm was measured using one iEEG signal. Line-length algorithm had the shortest processing time mainly due to its simplicity. Frequency homogeny algorithm needed more processing time but it was still faster than real time. Hilbert detection algorithm was approximately 5 times slower than real time suggesting that a compiled version of the algorithm should be developed in order to allow this algorithm to be used in clinic.

The line-length algorithm with simple post-processing steps (correlation and event to background ratio) showed very poor feature estimation yet the localization of SOZ was superior to other detectors. However, in localization of resected channels the algorithm performed poorly. With its speed this algorithm can be very useful in online HFO detection and use in clinic to give clinicians a rough idea about the HFO distribution in epileptic foci, thus highlighting the channels they should focus on.

Feature estimation error was the lowest for the Hilbert algorithm. This outcome demonstrates the algorithm's capability of HFO feature precise determination. Given the results in analysis of gold standard HFOs and pathologic tissue localization analysis this algorithm shows promising results that can be further improved by post-processing steps and machine learning methods.

Frequency homogeny algorithm showed the best performance in concordance with gold standard detections. Interestingly, the analysis of SOZ channel localization did not reveal good results but localization of resected channels was superior to line-length while inferior to Hilbert algorithm. As mentioned earlier in this work HFO marking is highly subjective. Enlarging the dataset on which the algorithm was trained is likely to improve the results. Feature estimation evaluation revealed that this detector can provide rough estimation of detected events' features.

7 DETECTION RESULT PRESENTATION

Conveying the results in simple and visually appealing way to the interpreter while preserving as much information as possible is crucial for wide spread usage of any detection algorithm in clinic and science. Consequently, development of result presentation is almost as important as the detection itself.

In this regard information acquired from the brain present a challenge. The electrophysiological signals have intrinsic features – amplitude and frequency. In case of HFOs, two other features can be acquired – duration and count. However, the physiology of the brain and its electrical properties change in time (cognition, sleep, etc.), space (neocortex, archicortex, etc.) and is dependent on external factors (drugs, external stimuli, etc.).

As it is apparent from the previous paragraph, it is not possible to visualize all information at once. Instead, the visualizations are focused on the desired application. Nonetheless, the interpreter should always be aware of the limitations.

7.1 HFO COUNT PER CHANNEL

Basic visualization used by vast majority of current publications dealing with HFO is usually a simple bar graph used to highlight channels with higher HFO occurrence. While this is sufficient for a general overview the loss of information about HFOs is significant. There is no information about HFO occurrence in time domain, which obstructs a potential feedback by medical staff or adjustment of medication. The frequency information is reduced to that of the frequency band used by algorithm filters. And the person reading the plot has to be aware of the individual contact locations within the brain in order to interpret the results correctly.

This type of visualization could stress the results by color-coding the HFO count in individual bars which would make it easier to identify the channels of interest. Furthermore, temporal information could be included by creating a video or by plotting numerous bar graphs for each time segment.

7.2 HFO COUNT WITH REGARD TO HFO FREQUENCY

This type of visualization was created as part of this PhD thesis and is useful for clinicians since fast ripples (250 – 600 Hz) are currently deemed to be correlated with pathologic brain more than ripples (80-250 Hz). The color-coded table presents HFO counts in individual frequencies and provide simplified information about the HFO distribution in frequency domain. The visualization was designed to present results of frequency homogeny algorithm, hence the frequency bands are set accordingly.

	44-62	52-73	62-86	73-102	86-121	102-143	121-169	143-199	169-237	199-280	237-332	280-392	332-464	392-549	464-650	549-769
A'1	8	4	22	40	6	22	43	53	37	21	1	1	0	0	0	1
A'2	7	1	22	6	3	4	9	3	3	12	13	4	0	0	0	0
A'3	15	4	21	17	10	18	45	39	22	11	2	0	1	0	0	0
A'4	7	9	16	9	22	33	27	24	36	30	4	0	7	2	0	0
A'5	12	2	16	11	13	20	18	12	53	46	7	4	8	3	0	0
A'6	5	3	16	6	13	19	11	8	79	48	7	2	4	2	0	0
A'7	4	3	14	5	7	17	11	5	44	34	14	5	4	1	0	0
A'8	7	11	21	9	8	11	13	0	7	4	3	2	0	0	0	0
A'9	11	7	19	10	7	7	7	2	1	1	4	2	0	0	0	0
A'10	10	3	8	4	3	2	6	1	5	8	9	1	0	1	0	0
B'1	12	11	50	104	69	42	86	94	133	172	81	35	34	14	0	0
B'2	8	6	12	14	5	11	11	4	7	3	0	0	0	0	0	0
B'3	10	11	22	31	36	47	108	160	243	296	171	123	128	58	1	0
B'4	13	7	17	16	14	33	85	123	217	263	154	101	120	46	0	0
B'5	6	4	6	8	5	30	77	89	144	94	31	4	7	1	0	0
B'6	9	5	25	8	4	11	22	11	19	13	5	2	1	1	0	0
B'7	14	3	36	12	7	16	44	10	16	8	0	0	0	2	0	0
B'8	20	3	22	17	4	11	14	3	1	0	0	0	0	1	0	0
B'9	13	5	17	5	5	12	18	2	6	0	0	0	0	1	0	0
B'10	2	6	14	9	5	12	12	2	2	0	0	0	0	1	0	0
B1	36	18	84	78	27	6	6	2	3	6	1	1	2	4	2	0
B2	14	6	10	9	10	17	24	2	14	19	15	6	1	3	1	0
B3	33	23	60	39	17	3	8	1	7	6	3	1	1	4	3	0
B4	41	29	60	24	5	3	6	3	4	9	3	3	2	6	3	0
B5	24	11	23	8	5	3	8	6	17	20	6	3	1	7	4	0
B6	9	3	13	8	2	5	10	4	9	9	4	2	1	5	3	0
B7	9	5	13	6	4	9	19	1	7	14	3	1	0	9	2	0
B8	11	4	10	8	8	4	19	3	13	19	8	8	1	5	4	0
B9	10	3	11	4	6	8	11	5	16	18	11	4	1	7	2	0
B10	9	10	9	6	7	5	7	7	12	22	12	6	1	5	4	0

Figure 4: ***Color-coded HFO rate in individual electrodes across frequencies.***

Image showing HFO occurrence in individual channels and in frequency bands with color-coded cells to stress the highest values. Color-coding contributes to simple immediate recognition of the areas with highest HFO rates.

Even though, this visualization provides fast overview about the tissue surrounding individual contacts there is still some information loss. Temporal aspect of HFO occurrence is completely neglected and information about HFO are represented solely by their count in frequency bands.

This type of visualization can be further developed by creating a video where changing colors would show shifts in HFO counts with regard to channels and frequency. This would account for temporal changes.

7.3 HFO COUNT WITH REGARD TO ANATOMY

Anatomical structure may play a crucial role in spatial distribution of HFO. It is, therefore, useful to visualize the information about HFO occurrence in MRI scans so that clinical staff has immediate information about the location of HFO generating tissue and can tie together the information of electrophysiology and anatomy of the particular patient's brain.

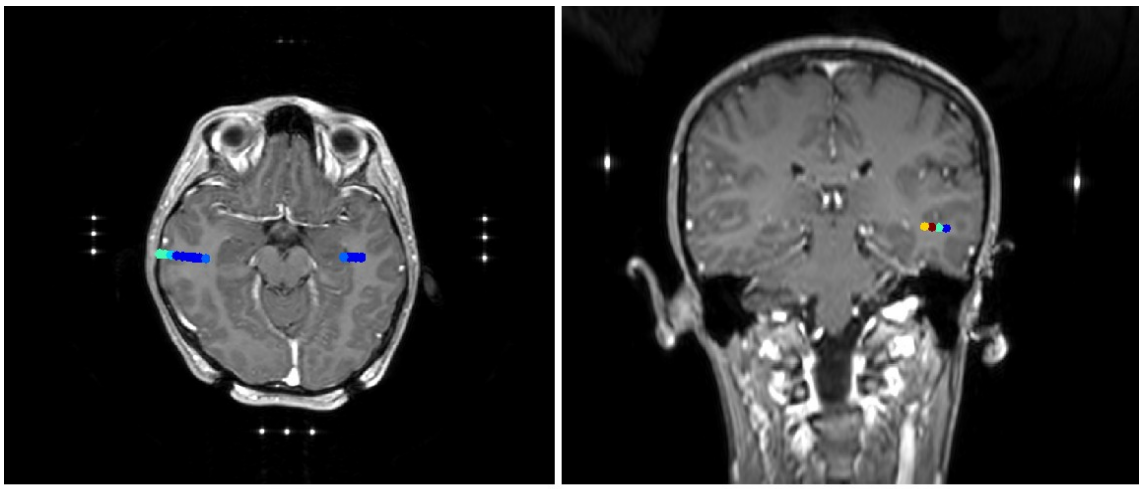

Figure 5: ***Color-coded HFO count in MRI slices.***

MRI scan of a patient with temporal lobe epilepsy. HFO counts are color coded as dots in places where electrode contacts were located. A – transversal plane B- coronal plane.

This method was created as a diploma thesis [34] which was mentored by the author of this work.

Further enhancements of this type of visualization can be again incorporation of information about HFO occurrence in time by creating video clips. Moreover, tractography analysis can be joined with this visualization in order to elucidate communication between different brain structures.

7.4 CIRCULAR GRAPHS

Inspired by data visualization in genome research, this type of graph reduces information loss to minimum while allowing for display of interactions between areas of the brain from which iEEG signal is acquired. The visualization was created within this work and is freely available as an open-source library which is being actively updated and developed (https://github.com/cimbi/pancircs) and can be easily installed through python package index.

Circular graphs can have multiple layers each expressing different piece of information. HFO counts and their mean attributes can be simply visualized this way although any type of electrophysiological information can be included such as spike rates or their features. Individual layers can also represent development of HFO occurrence in time, space and frequency.

Inner area of the circular graph can be used to visualize interactions between signals such as correlation or other connectivity metrics which can contribute to correct localization of pathologic tissue. Channels can be grouped according to their location in brain structures but any grouping variable can be used. Circles can be assembled into a series to create either an array or a video to capture the development of electrophysiological data in time.

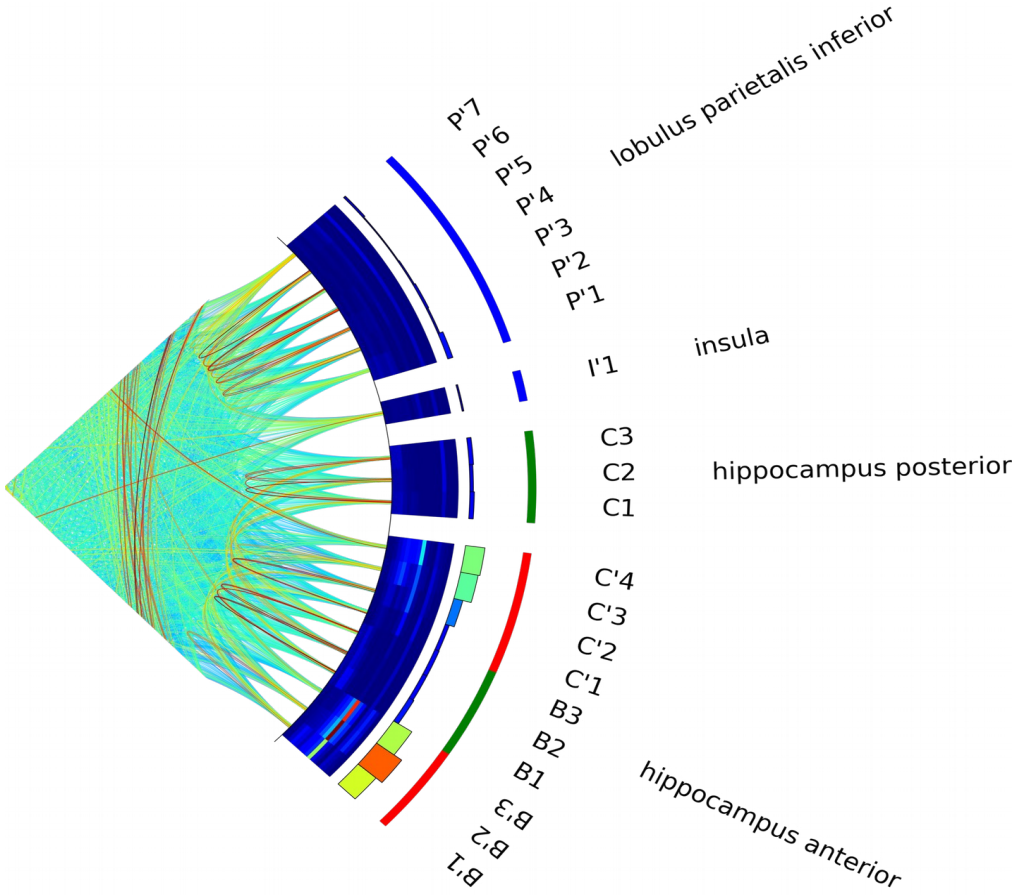

Figure 6: ***Circular visualization.***

Correlation between individual contacts (inner connections). Histogram of HFO count in frequency bands from low frequencies to high, inner to outer direction (inner circle). Total relative HFO count (middle circle). Pathology of channels (outer circle, SOZ -red, IZ – green, nonSOZ – blue). Contact sections are divided according to the structure in which they were located

CONCLUSION

High-frequency oscillations have been studied for over a decade now. All the studies conducted to date have proven that HFOs can indeed localize epileptogenic foci in focal epileptic patients and that by resecting pathological tissue with HFO a better surgical outcome can be achieved, leading to improvement of patients' lives. Nonetheless, most of the studies used retrospective visual or semiautomated detections of HFOs. Such approach is a time-consuming process and is prone to reviewer bias. An automated detection algorithm is needed as a fast and objective method of detection.

A number of HFO detectors have been developed to date at different institutions around the world. However, due to unclear definition of HFOs, their characteristics and different recording techniques, all detectors were trained and tested on different datasets. Moreover, evaluation of developed detectors is not uniform rendering the results of automated HFO detection incomparable.

The main aim of the presented work was to develop a robust detector which would be useful for physicians and provide them with additional information about the localization and spatial spread of epileptogenic focus. The secondary goal was to create a tool for research of HFO produced by pathological and healthy tissue as well as during different cognitive stages such as somatosensory processing or sleep and wake cycle.

Three HFO detection algorithms were developed or enhanced in this work. One is the line-length algorithm which was improved by post-processing steps, aims at use in clinic and has already been used to investigate the spatiotemporal dynamics of HFOs in patients with mesio-temporal epilepsy. The second is an algorithm based on a novel frequency homogeny metric that effectively reduces the false positive detections and takes human expertise into account through a set of boundary thresholds calculated from distribution functions created from visually marked HFOs. The last algorithm was developed for detailed HFO analysis with precise HFO feature estimation and is based on normalized amplitude envelopes and convolution of narrow band-passed signal and broad-band passed signal. Its earlier version has been already used for study of HFO behavior during cognitive task to investigate the normal function of the brain.

To test the feasibility of detectors from different points of view all detectors were subjected to three different evaluation methods designed to overcome the common drawbacks appearing in literature. To test agreement

with human reviewers the detections produced by automated methods were compared with gold standard detections created by manual review. Precision in HFO feature estimation was tested with artificial events inserted into iEEG signal and calculated feature values were compared with the known features of artificial events. Lastly, the ability to localize pathological tissue based on the count of HFO detections in individual channels was compared with clinically determined channels from which the seizures originated.

Results of evaluation confirmed effectiveness of each algorithm in the task they were designed for. While frequency homogeny algorithm had the best performance in agreement with gold standard detections, Hilbert algorithm showed the best feature estimation and localization of resected channels and line-length algorithm outperformed the remaining two in pathological tissue localization.

In order to convey the results to the end user, which is usually a clinician or a researcher, apt result visualization has to be chosen. Apart from wide-spread bar graph visualization of HFO count in individual channels, two other methods were developed in this work. One is a color-coded table with count in individual channels and frequency information. This allows clinicians to immediately evaluate the HFO analysis and is currently being used in St. Anne's University Hospital in Brno. The second method is inspired by visualization techniques in genome research and utilizes circular graphs. That allows for visualization of different HFO qualities as well as relationships between individual channels or brain structures.

The future work will focus on detector improvement and on combining their capabilities to provide better localization of pathological tissue while mapping the normal function of the brain. For that purpose more visually reviewed events will be acquired as well as data from multiple centers. HFO differentiation will be done with the use of machine learning methods and HFO spread will be studied with the use of brain connectivity methods and causality information. These future studies should improve both detection as well as general understanding of epilepsy and normal brain function.

All detection algorithms as well as evaluation codes mentioned in this work will be over time published online within the HFO-detect initiative (https://github.com/HFO-detect) that aims at creating a library of HFO detectors along with standardized evaluation tools. In conjunction with other algorithms developed around the world and publicly accessible iEEG

datasets this will allow for objective evaluation of each algorithm with precisely defined evaluation methods. Moreover, it will allow other centers around the world that have not yet started using HFOs in their research and in clinic to immediately begin automated detection in intracranial EEG and contribute with their datasets to the world wide pool. Circular visualization library is already available for easy installation through python package index (name: “pancircs”) and the source code is accessible on GitHub (https://github.com/cimbi/pancircs).

LITERATURE

[1] HOLDEN, E Wayne, Hoang THANH NGUYEN, Elizabeth GROSSMAN, Scott ROBINSON, Leila S NELSON, Margaret J GUNTER, Ann VON WORLEY and David J THURMAN. Estimating prevalence, incidence, and disease-related mortality for patients with epilepsy in managed care organizations. *Epilepsia* [online]. 2005, vol. 46, no. 2, pp. 311–9. ISSN 0013-9580. Available at: doi:10.1111/j.0013-9580.2005.30604.x

[2] WORRELL, Gregory A and Jean GOTMAN. High-frequency oscillations and other electrophysiological biomarkers of epilepsy: clinical studies. *Biomarkers in medicine* [online]. 2011, vol. 5, no. 5, pp. 557–66. ISSN 1752-0371. Available at: doi:10.2217/bmm.11.74

[3] BUZSÁKI, György, Z HORVÁTH, R URIOSTE, J HETKE and K WISE. High-frequency network oscillation in the hippocampus. *Science (New York, N.Y.)* [online]. 1992, vol. 256, no. 5059, pp. 1025–7. ISSN 0036-8075. Available at: http://www.ncbi.nlm.nih.gov/pubmed/1589772

[4] USUI, Naotaka, Kiyohito TERADA, Koichi BABA, Kazumi MATSUDA, Fumihiro NAKAMURA, Keiko USUI, Takayasu TOTTORI, Shuichi UMEOKA, Shigeru FUJITANI, Tadahiro MIHARA and Yushi INOUE. Very high frequency oscillations (over 1000 Hz) in human epilepsy. *Clinical Neurophysiology* [online]. 2010, vol. 121, no. 11, pp. 1825–1831 [accessed. 2013-10-18]. ISSN 1872-8952. Available at: doi:10.1016/j.clinph.2010.04.018

[5] RAY, Supratim, Nathan E CRONE, Ernst NIEBUR, Piotr J FRANASZCZUK and Steven S HSIAO. Neural correlates of high-gamma oscillations (60-200 Hz) in macaque local field potentials and their potential implications in electrocorticography. *The Journal of neuroscience : the official journal of the Society for Neuroscience* [online]. 2008, vol. 28, pp. 11526–11536. ISSN 0270-6474. Available at: doi:10.1523/JNEUROSCI.2848-08.2008

[6] WILSON, M A and B L MCNAUGHTON. Reactivation of hippocampal ensemble memories during sleep. *Science (New York, N.Y.)* [online]. 1994, vol. 265, pp. 676–679. ISSN 0036-8075. Available at: doi:10.1126/science.8036517

[7] SULLIVAN, David, Jozsef CSICSVARI, Kenji MIZUSEKI, Sean MONTGOMERY, Kamran DIBA and György BUZSÁKI. Relationships between hippocampal sharp waves, ripples, and fast gamma oscillation: influence of dentate and entorhinal cortical activity. *The Journal of neuroscience : the official journal of the Society for Neuroscience* [online]. 2011, vol. 31, pp. 8605–8616. ISSN 0270-6474. Available at: doi:10.1523/JNEUROSCI.0294-11.2011

[8] BRAGIN, Anatol, J ENGEL, C L WILSON, I FRIED and György BUZSÁKI. High-frequency oscillations in human brain. *Hippocampus* [online]. 1999, vol. 9, no. 2, pp. 137–42. ISSN 1050-9631. Available at: doi:10.1002/(SICI)1098-1063(1999)9:2<137::AID-HIPO5>3.0.CO;2-0

[9] BRAGIN, Anatol, Jerome ENGEL, Charles L WILSON, Itzhak FRIED and Gary W. MATHERN. Hippocampal and entorhinal cortex high-frequency oscillations (100--500 Hz) in human epileptic brain and in kainic acid--treated rats with chronic seizures. *Epilepsia* [online]. 1999, vol. 40, no. 2, pp. 127–37 [accessed. 2013-10-28]. ISSN 0013-9580. Available at: doi:10.1111/j.1528-1157.1999.tb02065.x

[10] STABA, Richard J, Charles L WILSON, Anatol BRAGIN, Itzhak FRIED and Jerome ENGEL. Quantitative Analysis of High-Frequency Oscillations (80 − 500 Hz) Recorded in Human Epileptic Hippocampus and Entorhinal Cortex. *Journal of neurophysiology*. 2002, vol. 88, pp. 1743–1752.

[11] URRESTARAZU, Elena, Jeffrey D JIRSCH, Pierre LEVAN, Jeffery HALL, Massimo AVOLI, Francois DUBEAU and Jean GOTMAN. High-frequency intracerebral EEG activity (100-500 Hz) following interictal spikes. *Epilepsia* [online]. 2006, vol. 47, no. 9, pp. 1465–76 [accessed. 2014-01-20]. ISSN 0013-9580. Available at: doi:10.1111/j.1528-1167.2006.00618.x

[12] WORRELL, Gregory A, Andrew B GARDNER, S Matt STEAD, Sanqing HU, Steve GOERSS, Gregory J CASCINO, Fredric B MEYER, Richard MARSH and Brian LITT. High-frequency oscillations in human temporal lobe: simultaneous microwire and clinical macroelectrode recordings. *Brain* [online]. 2008, vol. 131, no. Pt 4, pp. 928–937. Available at: doi:10.1093/brain/awn006.High-frequency

[13] JACOBS, Julia, Pierre LEVAN, Rahul CHANDER, Jeffery HALL, François DUBEAU and Jean GOTMAN. Interictal high-frequency oscillations (80-500 Hz) are an indicator of seizure onset areas independent of spikes in the human epileptic brain. *Epilepsia* [online]. 2008, vol. 49, no. 11, pp. 1893–907 [accessed. 2014-01-09]. ISSN 1528-1167. Available at: doi:10.1111/j.1528-1167.2008.01656.x

[14] JACOBS, Julia, Pierre LEVAN, Claude-Edouard CHÂTILLON, André OLIVIER, François DUBEAU and Jean GOTMAN. High frequency oscillations in intracranial EEGs mark epileptogenicity rather than lesion type. *Brain : a journal of neurology* [online]. 2009, vol. 132, no. Pt 4, pp. 1022–37 [accessed. 2013-11-25]. ISSN 1460-2156. Available at: doi:10.1093/brain/awn351

[15] BAGSHAW, Andrew P, Julia JACOBS, Pierre LEVAN, François DUBEAU and Jean GOTMAN. Effect of sleep stage on interictal high-frequency oscillations recorded from depth macroelectrodes in patients with focal epilepsy. *Epilepsia* [online]. 2009, vol. 50, no. 4, pp. 617–28 [accessed. 2014-01-22]. ISSN 1528-1167. Available at: doi:10.1111/j.1528-1167.2008.01784.x

[16] BRÁZDIL, Milan, Josef HALÁMEK, Pavel JURÁK, Pavel DANIEL, Robert KUBA, Jan CHRASTINA, Zdenek NOVÁK and Ivan REKTOR. Interictal high-frequency oscillations indicate seizure onset zone in patients with focal cortical dysplasia. *Epilepsy research* [online]. 2010, vol. 90, no. 1-2, pp. 28–32 [accessed. 2014-01-22]. ISSN 1872-6844. Available at: doi:10.1016/j.eplepsyres.2010.03.003

[17] CRÉPON, Benoît, Vincent NAVARRO, Dominique HASBOUN, Stéphane CLEMENCEAU, Jacques MARTINERIE, Michel BAULAC, Claude ADAM and Michel LE VAN QUYEN. Mapping interictal oscillations greater than 200 Hz recorded with intracranial macroelectrodes in human epilepsy. *Brain : a journal of neurology* [online]. 2010, vol. 133, no. Pt 1, pp. 33–45 [accessed. 2014-01-22]. ISSN 1460-2156. Available at: doi:10.1093/brain/awp277

[18] JACOBS, Julia, Maeike ZIJLMANS, Rina ZELMANN, Claude-Edouard CHATILLON, Jeffrey HALL, André OLIVIER, François DUBEAU and Jean GOTMAN. High-frequency electroencephalographic oscillations correlate with outcome of epilepsy surgery. *Annals of neurology* [online]. 2010, vol. 67, no. 2, pp. 209–20 [accessed. 2014-01-11]. ISSN 1531-8249. Available at: doi:10.1002/ana.21847

[19] WU, J Y, R SANKAR, J T LERNER, Joseph Y MATSUMOTO, H V VINTERS and G W MATHERN. Removing interictal fast ripples on electrocorticography linked with seizure freedom in children. *Neurology* [online]. 2010, vol. 75, no. 19, pp. 1686–94 [accessed. 2014-01-29]. ISSN 1526-632X. Available at: doi:10.1212/WNL.0b013e3181fc27d0

[20] BLANCO, Justin A, S Matt STEAD, Abba KRIEGER, Jonathan VIVENTI, W Richard MARSH, Kendall H LEE, Gregory A WORRELL and Brian LITT. Unsupervised classification of high-frequency oscillations in human neocortical epilepsy and control patients. *Journal of neurophysiology* [online]. 2010, vol. 104, no. 5, pp. 2900–2912 [accessed. 2013-10-24]. ISSN 1522-1598. Available at: doi:10.1152/jn.01082.2009

[21] NELSON, Ryan, Stephen M MYERS, Jennifer D SIMONOTTO, Michael D FURMAN, Mark SPANO, Wendy M NORMAN, Zhao LIU, Thomas B DEMARSE, Paul R CARNEY and William L DITTO. Detection of high frequency oscillations with Teager energy in an animal model of limbic epilepsy. In: *Conference proceedings : ... Annual International Conference of the IEEE Engineering in Medicine and Biology Society. IEEE Engineering in Medicine and Biology Society. Conference*. 2006, p. 2578–2580. ISBN 1424400333.

[22] MARAGOS, Petros, James F. KAISER and Thomas F. QUATIERI. On Amplitude and Frequency Demodulation Using Energy Operators. *Transactions on signal processing*. 1993, vol. 41, no. 4, pp. 1532–1550.

[23] GARDNER, Andrew B, Gregory A WORRELL, Eric MARSH, Dennis DLUGOS and Brian LITT. Human and automated detection of high-frequency oscillations in clinical intracranial EEG recordings. *Clinical Neurophysiology* [online]. 2007, vol. 118, pp. 1134–1143. Available at: http://ac.els-cdn.com/S1388245707000399/1-s2.0-S1388245707000399-main.pdf?_tid=8d8f837c-495a-11e3-bf45-00000aab0f27&acdnat=1384014082_e4c6ec289ef5c4698503b2a7c2ee0bbc

[24] ZELMANN, Rina, F MARI, Julia JACOBS, Maeike ZIJLMANS, Rahul CHANDER and J GOTMAN. Automatic detector of High Frequency Oscillations for human recordings with macroelectrodes. In: *32nd Annual International Conference of the IEEE EMBS*. 2010, p. 2329–2333. ISBN 9781424441242.

[25] DÜMPELMANN, Matthias, Julia JACOBS, Karolin KERBER and Andreas SCHULZE-BONHAGE. Automatic 80-250Hz 'ripple' high frequency oscillation detection in invasive subdural grid and strip recordings in epilepsy by a radial basis function neural network. *Clinical neurophysiology : official journal of the International Federation of Clinical Neurophysiology* [online]. 2012, vol. 123, no. 9, pp. 1721–31 [accessed. 2016-01-16]. ISSN 1872-8952. Available at: doi:10.1016/j.clinph.2012.02.072

[26] LÓPEZ-CUEVAS, Armando, Bernardino CASTILLO-TOLEDO, Laura MEDINA-CEJA, Consuelo VENTURA-MEJÍA and Kenia PARDO-PEÑA. An algorithm for on-line detection of high frequency oscillations related to epilepsy. *Computer methods and programs in biomedicine* [online]. 2013, vol. 110, no. 3, pp. 354–60 [accessed. 2013-10-26]. ISSN 1872-7565. Available at: doi:10.1016/j.cmpb.2013.01.014

[27] PINCUS, Steven M. Approximate entropy as a measure of system complexity. In: *Proceedings of National Academy of Sciences 1991*. no date.

[28] LIANG, Sheng-Fu, Kuo-Tien LEE, Yu-Hsiang PAN and Yung-Hung WANG. Fast computation of sample entropy and approximate entropy in biomedicine. *Computer Methods and Programs in Biomedicine* [online]. 2011, vol. 104, no. 3, pp. 382–396 [accessed. 2013-10-26]. ISSN 1872-7565. Available at: doi:10.1016/j.cmpb.2010.12.003

[29] CHAIBI, Sahbi, Zied SAKKA, Tarek LAJNEF, Mounir SAMET and Abdennaceur KACHOURI. Automated detection and classification of high frequency oscillations (HFOs) in human intracereberal EEG. *Biomedical Signal Processing and Control* [online]. 2013, vol. 8, no. 6, pp. 927–934 [accessed. 2014-02-14]. ISSN 17468094. Available at: doi:10.1016/j.bspc.2013.08.009

[30] BIROT, Gwénaël, Amar KACHENOURA, Laurent ALBERA, Christian BÉNAR and Fabrice WENDLING. Automatic detection of fast ripples. *Journal of neuroscience methods* [online]. 2013, vol. 213, no. 2, pp. 236–49 [accessed. 2016-01-16]. ISSN 1872-678X. Available at: doi:10.1016/j.jneumeth.2012.12.013

[31] BURNOS, Sergey, Peter HILFIKER, Oguzkan SÜRÜCÜ, Felix SCHOLKMANN, Niklaus KRAYENBÜHL, Thomas GRUNWALD and Johannes SARNTHEIN. Human intracranial high frequency oscillations (HFOs) detected by automatic time-frequency analysis. *PloS one* [online]. 2014, vol. 9, no. 4, p. e94381 [accessed. 2016-01-16]. ISSN 1932-6203. Available at: doi:10.1371/journal.pone.0094381

[32] ZELMANN, Rina, F MARI, Julia JACOBS, Maeike ZIJLMANS, François DUBEAU and Jean GOTMAN. A comparison between detectors of high frequency oscillations. *Clinical Neurophysiology* [online]. 2012, vol. 123, no. 1, pp. 106–116 [accessed. 2013-10-26]. ISSN 1872-8952. Available at: doi:10.1016/j.clinph.2011.06.006

[33] DÜMPELMANN, Matthias, Julia JACOBS, Karolin KERBER and Andreas SCHULZE-BONHAGE. Automatic 80-250Hz 'ripple' high frequency oscillation detection in invasive subdural grid and strip recordings in epilepsy by a radial basis function neural network. *Clinical neurophysiology : official journal of the International Federation of Clinical Neurophysiology* [online]. 2012, vol. 123, no. 9, pp. 1721–31. ISSN 1872-8952. Available at: doi:10.1016/j.clinph.2012.02.072

[34] TRAVNICEK, Vojtech. *Interactive spatial visualisation of eeg parameters from depth intracranial electrodes in CT/MRI images*. B.m., 2015. Brno University of Technology.